CrystEngComm

Accepted Manuscript

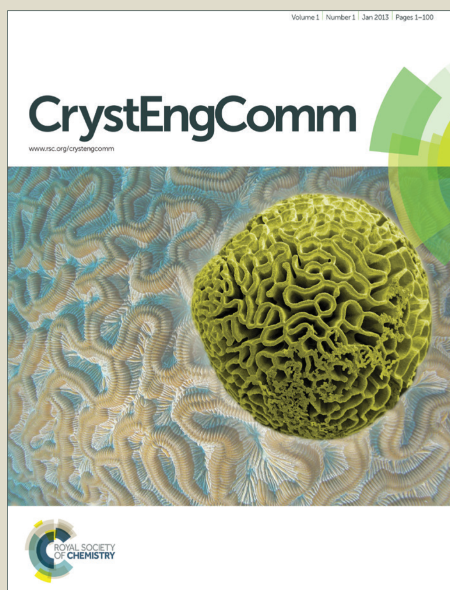

This is an *Accepted Manuscript*, which has been through the Royal Society of Chemistry peer review process and has been accepted for publication.

Accepted Manuscripts are published online shortly after acceptance, before technical editing, formatting and proof reading. Using this free service, authors can make their results available to the community, in citable form, before we publish the edited article. We will replace this *Accepted Manuscript* with the edited and formatted *Advance Article* as soon as it is available.

You can find more information about *Accepted Manuscripts* in the Information for Authors.

Please note that technical editing may introduce minor changes to the text and/or graphics, which may alter content. The journal's standard Terms & Conditions and the Ethical guidelines still apply. In no event shall the Royal Society of Chemistry be held responsible for any errors or omissions in this *Accepted Manuscript* or any consequences arising from the use of any information it contains.

ROYAL SOCIETY OF CHEMISTRY

www.rsc.org/crystengcomm

CrystEngComm

Dynamic Article Links ►

Cite this: DOI: 10.1039/c0xx00000x

www.rsc.org/xxxxxx

COMMUNICATION

Growth of single-crystalline nickel silicide nanowires with excellent physical properties

Jen-Yi Lin[a], Hsiu-Ming Hsu[a], and Kuo-Chang Lu *[a,b]

Received (in XXX, XXX) Xth XXXXXXXXX 20XX, Accepted Xth XXXXXXXXX 20XX
DOI: 10.1039/b000000x

Single-crystalline $NiSi_2$, Ni_2Si and $Ni_{31}Si_{12}$ nanowire arrays coated with amorphous silicon dioxide were synthesized with high quality and quantity by nickel transported chemical vapor deposition (CVD) method. The morphological changes with various reaction temperatures, ambient pressures and reaction times, were observed and studied, respectively. At 750°C and 850°C, cone-shaped nanowire arrays were formed, composed of dense and oriented $Ni_{31}Si_{12}$ and Ni_2Si nanowires with length of over 60μm. The growth mechanisms of the nickel silicide nanowires have been proposed and identified with microscopy studies. Field emission measurements show that the as-grown $NiSi_2$, Ni_2Si and $Ni_{31}Si_{12}$ nanowires were of remarkable field enhancement factors, 2532, 4822 and 4099, respectively, and magnetic property measurements show a ferromagnetic characteristic for Ni_2Si and $Ni_{31}Si_{12}$ nanowires, demonstrating promising potential applications for field emitters, magnetic storage, and biological cell separation.

Introduction

As the trend of device-miniaturization continues, people are seeking for semiconducting nanowire materials of free-standing growth and excellent physical properties. Nickel silicide nanowires stir widespread investigations due to their applications in future nanoelectronic devices[1-4]. Also, their outstanding field emission and magnetic properties make them attractive choices for nanoscale field emitters[5, 6] and biological applications[7]. Over decades, numerous phases of nickel silicide nanowires have been synthesized through various approaches, which may be classified into three categories: (1) silicidation of silicon nanowires[1, 2, 8-10] (2) Si transported method[5, 6, 11-16] (3) chemical vapor transport(CVT) method[17, 18]. Notably, most of the synthesis strategies were silicon transported and strongly depend on the very fast diffusion rate of nickel atoms in silicon[19]. However, nickel transported synthesis method with silicon diffusion has not been studied.

In this work, various nickel silicides with excellent field emission were synthesized via nickel transported chemical vapor deposition method using $NiCl_2•6H_2O$ as a single precursor. The effects of growth temperature and ambient pressure on the morphology of nanowires have been discussed. The growth mechanism and the growth steps have been studied as well. It is worth mentioning that the key factors of growth of the nickel silicide nanowires here were silicon diffusion rate and nickel deposition rate. Moreover, the ferromagnetic properties of Ni_2Si and $Ni_{31}Si_{12}$ were demonstrated, which may contribute to biological applications.

Experimental Methods

Single crystalline (001) silicon substrates were pre-cleaned in acetone and isopropanol by ultrasonic vibration, followed by dilute hydrofluoric (HF) dipping to remove native oxide, cleaning with deionized water and drying with N_2. The cleaned Si substrates were transferred into the downstream of a horizontal hot-wall furnace for chemical vapor deposition (CVD) process. Nickel (II) chloride hexahydrate powder (99.9%) of 0.4g was placed in an aluminum boat at the upstream of the furnace as a precursor. The precursor temperature and the growth temperature were annealed to 600°C and 400-950°C, respectively, at a ramping rate of 0.5°C/sec and the growth time was fixed at 30min. 99.9% argon gas was introduced into the furnace at a flow rate of 30sccm for supporting the transportation of the precursor. The ambient pressure was controlled by argon partial pressure and maintained at 10torr. The morphology observation was carried out by field emission scanning electron microscope (FESEM) (Hitachi SU8000 with an acceleration voltage of 15kV). Spherical aberration corrected scanning transmission electron microscope (Cs-corrected STEM) (JEOL ARM200F operating at 200kV) equipped with energy dispersive spectroscopy and X-ray diffractometer (XRD) were utilized for structural characterization, phase identification and atomic ratio analysis. Field emission properties were measured in a vacuum chamber equipped with a Keithley power supply. Magnetic property measurements were conducted by superconducting quantum interference device vibrating sample magnetometer (SQUID VSM).

CrystEngComm Accepted Manuscript

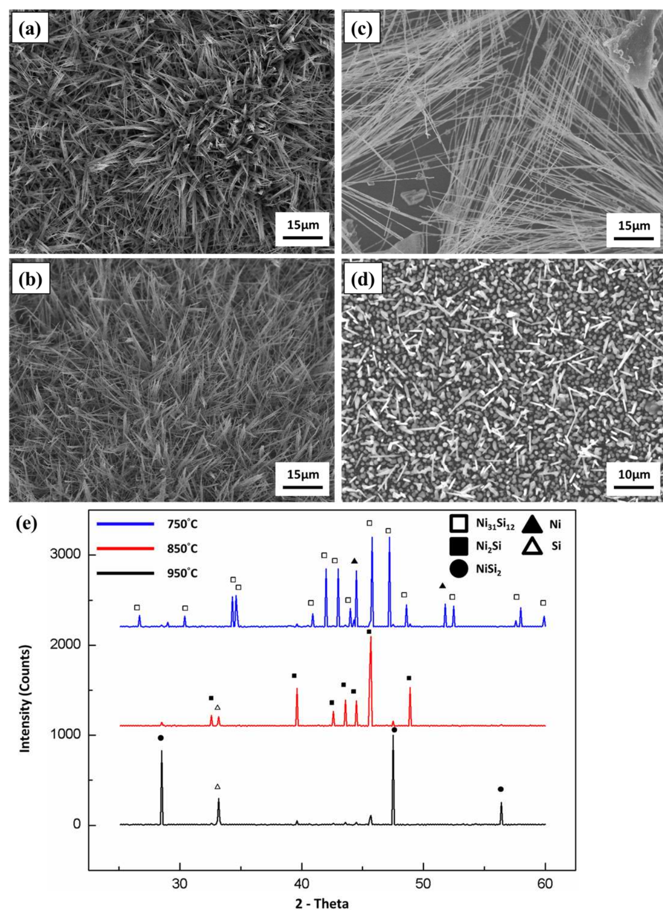

Fig. 1 SEM images of nickel silicide nanowires grown on (100) Si substrates at (a)750°C, (b)850°C, (c)950°C, respectively. (d) Ni nanowires grown on a (100) Si substrate at 400°C and 70torr. (e) XRD analysis for nickel silicide nanowires grown on (100) Si substrates at 750°C, 850°C and 950°C, respectively.

Results and discussion

Morphologies and TEM analysis

Fig. 1(a)-(c) show SEM images of as-grown nanowires at 750°C, 850°C and 950°C, respectively. High density nanowire arrays with length of over 60μm were observed at 750°C and 850°C. Most of the nanowires tended to grow vertically with respect to silicon substrates. For samples grown at 950°C, nanowires tended to grow horizontally with a lower density and length of over 100μm; longer NWs tended to grow parallelly. This may be attributed to the fact that the increasing weight with the increasing length of a single NW can no longer be supported by the root, leading to the horizontal growth of the NW. The diameters of the nanowires ranged from 15-40nm, which indicates that the as-grown nanostructures possess a great aspect ratio of over 2500. XRD analysis of the samples at growth temperatures of 750°C -950°C was shown in Fig. 1(e). The diffraction peaks of 750°C sample are for $Ni_{31}Si_{12}$ phase; at 850°C, the peaks mainly correspond to Ni_2Si phase; at 950°C, $NiSi_2$ peaks were dominating. Fig. 1(d) shows the nanowire sample grown at 400°C and

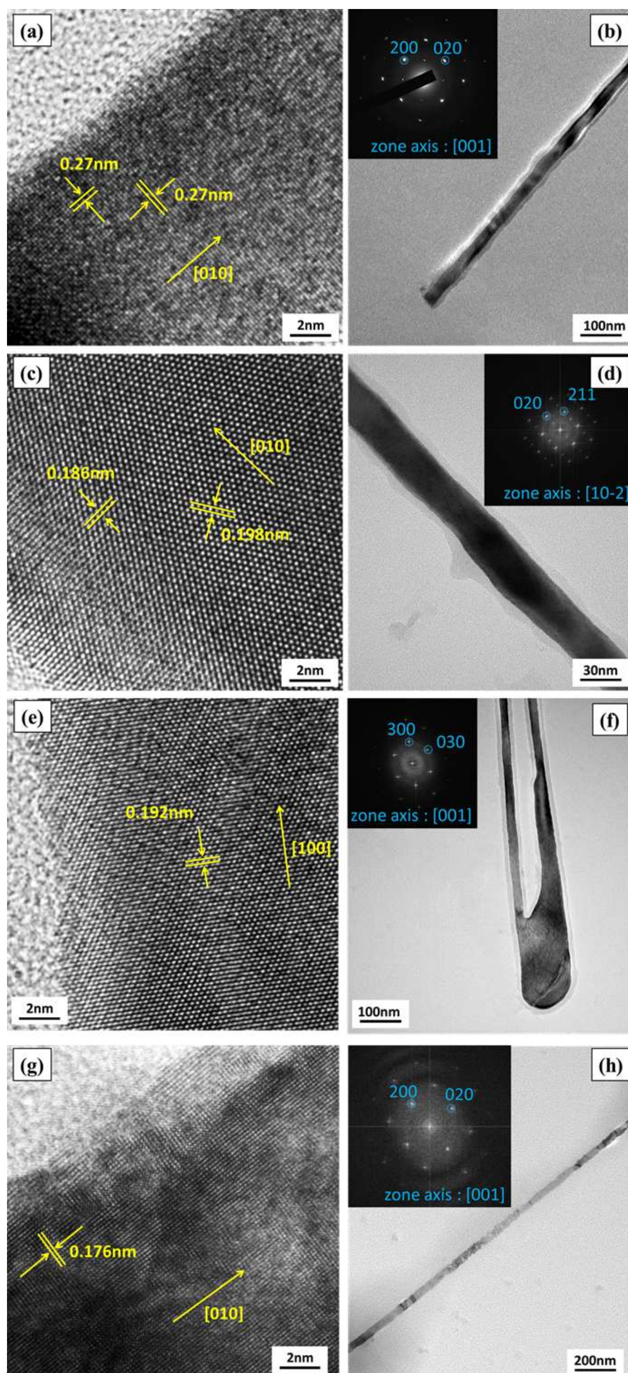

Fig. 2 Low-magnification, high-resolution TEM images and selected area /FFT diffraction patterns of (a), (b) $NiSi_2$ (c), (d) Ni_2Si (e), (f) $Ni_{31}Si_{12}$ (g), (h) Ni nanowires grown on (100)Si substrates at 950°C, 850°C, 750°C, 400°C, respectively.

70torr, where only Ni peaks were detected based on the XRD analysis.

On structural characterization, Fig. 2 shows TEM images, HRTEM images, and selected area or fast Fourier transform (FFT) diffraction patterns of the nanowires grown at different temperatures. Fig. 2(b) shows a $NiSi_2$ nanowire at 950°C; on the basis of the HRTEM image in Fig. 2(a) and the corresponding selected area diffraction pattern in the inset of Fig. 2(b), the structure of the material has been determined to be single crystal $NiSi_2$ of a face-

CrystEngComm Accepted Manuscript

This journal is © The Royal Society of Chemistry [year]

centered cubic structure with a lattice constant of 0.5406 nm. Fig. 2(d) shows a Ni_2Si nanowire at 850°C; from the HRTEM image in Fig. 2(c) and the corresponding FFT diffraction pattern in the inset of Fig. 2(d), the material was identified to be single crystal δ-Ni_2Si of an orthorhombic structure with lattice constants of a = 0.499 nm, b = 0.372 nm, and c = 0.703 nm. Fig. 2(f) shows a $Ni_{31}Si_{12}$ nanowire at 750°C; based on the HRTEM image in Fig. 2(e) and the corresponding FFT diffraction pattern in the inset of Fig. 2(f), the single crystalline material was identified to be hexagonal $Ni_{31}Si_{12}$ with lattice constants of a = 0.6667 nm and c = 1.2277 nm. At 400°C, Ni nanowires were observed. All of the nanowires were of core-shell structures with a SiO_2 shell and a silicide core, which is consistent with the EDS analysis. The growth direction of the $NiSi_2$, Ni_2Si and Ni NWs was [010], while that of the $Ni_{31}Si_{12}$ NWs was [100]. Notably, as the growth temperature decreased, nickel silicides of nickel-rich phases appeared. This may result from the decrease of the growth temperature facilitating the supersaturation of the precursor, which modified the growth environment to favor formation of Ni-rich phases. Also, this is coherent with the Ni-Si phase diagram, where Ni-rich phases, Ni_2Si and $Ni_{31}Si_{12}$, appear.

Growth mechanisms

At 850°C, the variation of nanowire morphologies among different ambient pressures was shown in Fig. 3(a)-(c). At 5torr (Figure 3(a)), the as-grown sample was mainly composed of nickel silicide bulk and island structures with scattered growth of nanowires. The optimum ambient pressure was 10torr as shown in Fig. 3(b), where the sample was covered with cone-shape nanowire arrays, composed of nanowire groups with highly consistent growth directions. In Fig. 3(c), as the pressure was increased to 15torr, the density of the NWs apparently decreased, which exposed some Si substrates; however, nanowire groups with consistent growth directions were still observed. The cause of the decreasing growth density may be explained by the effect of argon concentrations. Since the ambient pressure was controlled by varying the partial pressure of argon, with the increase of the ambient pressure, the concentration of argon in the furnace increased and so did the frequency of collision among argon and precursor molecules, which impeded the vaporization of precursor molecules and decreased the supersaturation of Ni. Furthermore, it can be found that the diameter increased with the ambient pressure. The relation between the change of unit volume free energy and critical radius of the nuclei during the nanowire nucleation process is based on the equation below:

$$r_c = -\frac{2\sigma}{\Delta G_v},$$

where r_c is the critical radius of the nuclei, σ is the unit surface free energy, and ΔG_v is the change of unit volume free energy[20]. Since the nanowire nucleation is a supersaturation condensation reaction, ΔG_v can be expressed as a function of temperature and supersaturation of the precursor:

$$\Delta G_v = -\frac{k_B T}{v} \ln \frac{P_{ssat}}{P_0},$$

where P_{ssat}/P_0 is the supersaturation of precursor at T, k_B is the Boltzmann constant, and v is the molar volume of the nuclei[20]. After derivation, the relation between r_c and supersaturation would be:

$$r_c = \frac{2v\sigma}{kT \ln P_{ssat}/P_0},$$

From here, as the ambient pressure increases, P_{ssat}/P_0 would decrease; thus, r_c becomes larger. This explains the findings[21]. From the observation above, we propose the growth process shown in Fig. 4. Firstly, Ni was deposited on Si substrates, forming interfaces between Ni and Si for further reactions. Ni deposition could happen via thermal decomposition of precursors:

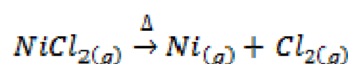

$$NiCl_{2(g)} \xrightarrow{\Delta} Ni_{(g)} + Cl_{2(g)}$$

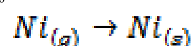

$$Ni_{(g)} \rightarrow Ni_{(s)}$$

Also, nickel silicide particles could directly form by reacting with Si substrates through the paths shown below:
At 850°C,

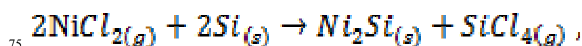

$$2NiCl_{2(g)} + 2Si_{(s)} \rightarrow Ni_2Si_{(s)} + SiCl_{4(g)},$$

$$2NiCl_{2(g)} + SiCl_{4(g)} \rightarrow Ni_2Si_{(s)} + 4Cl_{2(g)},$$

At 950°C,

$$2NiCl_{2(g)} + 5Si_{(s)} \rightarrow 2NiSi_{2(s)} + SiCl_{4(g)},$$

$$NiCl_{2(g)} + 2SiCl_{4(g)} \rightarrow NiSi_{2(s)} + 5Cl_{2(g)},$$

Secondly, Si and Ni reacted to form nickel silicide bulk and island structures. In addition to the deposition of Ni, a concentration gradient formed, providing driving energy for Si atoms to diffuse to the reaction area around the surface through the nickel silicide region in the substrates simultaneously. As the supply of Si and Ni atoms remained, nickel silicide NWs nucleated and grew from the islands and platforms. The consistent direction was due to the epitaxial growth on the same platform.

Field emission measurements of the nickel silicide nanowires

In addition to understanding the growth behaviors of the nickel silicide nanowires, we explored the physical properties of them and etched away the oxide shell before measurements. Fig. 5 shows field emission properties of $Ni_{31}Si_{12}$, Ni_2Si, and $NiSi_2$ NWs, respectively, with insets of corresponding ln (J/E^2)-$(1/E)$ plots. The samples were measured at pressure of about 10^{-5} torr and the distance between the anode and emitting surface was fixed at 100μm. The turn-on field was defined as the applied field attained for a current density of 10μA/cm^2 and was found to be about 2.39V/μm, 2.28V/μm and 2.64V/μm for $Ni_{31}Si_{12}$, Ni_2Si and $NiSi_2$, respectively. The field emission

CrystEngComm Accepted Manuscript

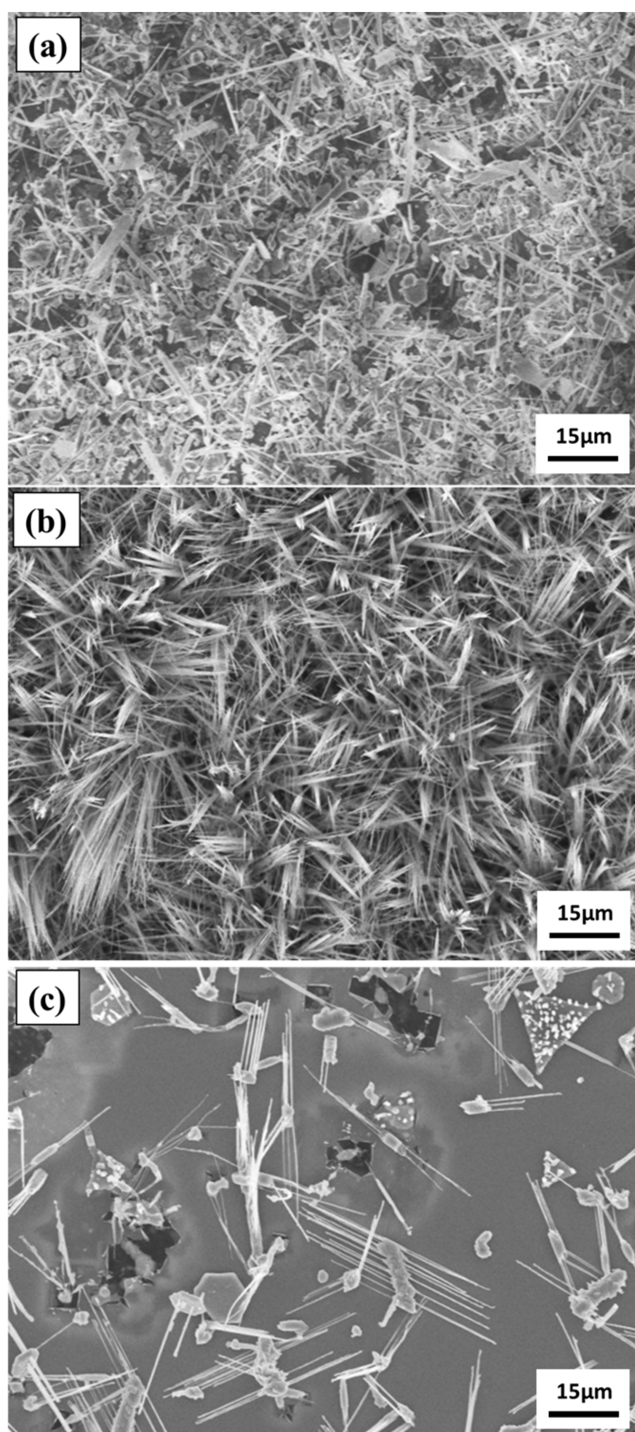

Fig. 3 SEM images of Ni_2Si nanowires grown on (100) Si substrates at (a)5torr, (b)10torr, (c)15torr, respectively.

behavior can be described by the following equation derived from the Fowler-Nordheim (F-N) relationship:

$$\ln(J/E^2) - \ln(A\beta^2/\varphi) = -B\varphi^{3/2}/\beta E\ ,$$

where J is the field emission current density, E is the applied electric field strength, β is the field enhancement factor, φ is the work function of the as-grown nanowires, and the universal constants $A= 1.54 \times 10^{-10}$ $(AV^{-2}\bullet eV)$ and $B= 6.83 \times 10^3$ $(eV^{-3/2}\ V\bullet \mu m^{-1})$[22]. By calculating the slopes of $\ln(J/E^2)$–$(1/E)$ plots with work function values of $Ni_{31}Si_{12}$ (4.8 eV), Ni_2Si (4.8 eV), and $NiSi_2$ (4.7eV)[23, 24],

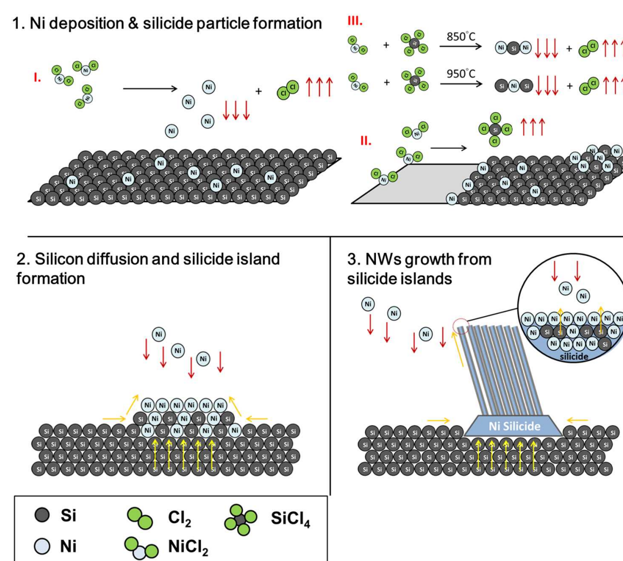

Fig. 4 Schematic illustration of the growth mechanisms.

the field enhancement factor β has been determined to be 4099, 4822 and 2532, respectively, which is better than previous reports and supports the development of field emitter devices[5, 6]. The great performance of the field emission properties was attributed to their metallic property, special one dimensional geometry with a high aspect ratio and cone-shape morphology. A cone is composed of numerous highly dense and well-aligned nanowires, believed to contribute to the high field-enhancement.

Magnetic property measurements of the nickel silicide nanowires

We measured the magnetic properties for the nickel silicide nanowires with SQUID at 2K as shown in Fig. 6. $NiSi_2$ NWs were found to be diamagnetic, while Ni_2Si and $Ni_{31}Si_{12}$ NWs were ferromagnetic; the coercivities of the former and the latter were 135Oe and 417Oe; the saturation magnetizations of the former and the latter were 0.12emu and 0.26emu, respectively. It is known that silicon is a diamagnetic material, while nickel is a ferromagnetic material with unit volume saturation magnetization of about 484emu/cm^3; thus, the relationship between nickel silicide nanowires with different Ni/Si atomic ratios has been investigated. Based on our experimental results on magnetic properties, as the Ni/Si ratio of the silicide NWs increased, both coercivity and saturation magnetization became larger, which demonstrated the positive correlation between the nickel silicide at nanoscale and the Ni/Si ratio. From this study, the synthesized Ni_2Si and $Ni_{31}Si_{12}$ nanowires with ferromagnetic properties could provide potential applications in the biological field.

Conclusions

Single crystalline $NiSi_2$, Ni_2Si, and $Ni_{31}Si_{12}$ nanowire arrays were successfully synthesized with Ni transported

CrystEngComm Accepted Manuscript

This journal is © The Royal Society of Chemistry [year]

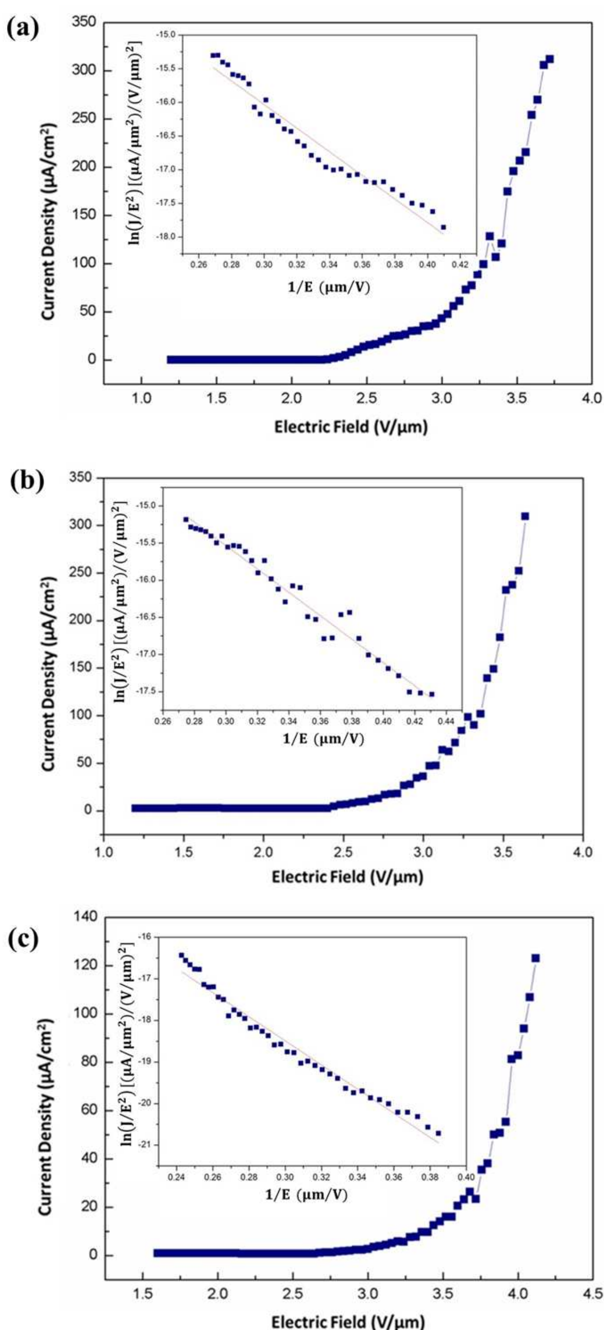

Fig. 5 Field emission plots for nickel silicide nanowires of different phases with insets of corresponding ln (J/E^2)-(1/E) plots at (a)750°C (b)850°C (c) 950°C.

$NiCl_2 \cdot 6H_2O$ as a single precursor. By varying and controlling the growth conditions, dense $NiSi_2$, Ni_2Si, $Ni_{31}Si_{12}$ nanowire arrays with highly consistent growth directions were fabricated at source temperature of 600°C, ambient pressure of 10torr and growth temperature of 950°C, 850°C and 750°C, respectively. Additionally, we have proposed the growth mechanisms and reaction paths based on SEM, TEM and XRD studies. Electrical measurements show that the nickel silicide nanowires exhibited excellent field emission property, making them attractive candidates for emitting materials with a low

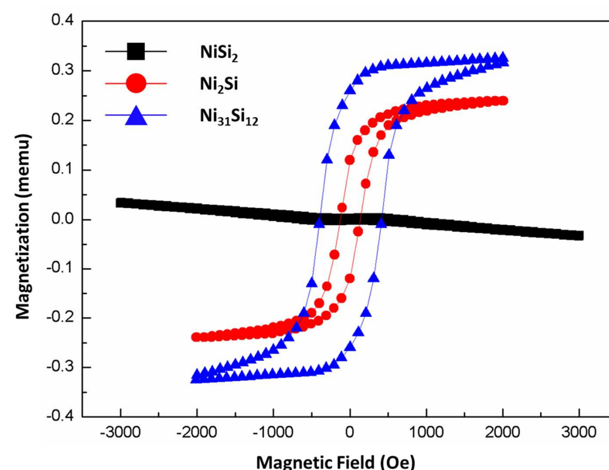

Fig. 6 Plots of M-H curve at 2K for nickel silicide nanowires of three different phases.

turn-on field. Magnetic measurements via SQUID show the ferromagnetic property of the $Ni_{31}Si_{12}$ and Ni_2Si nanowires. This work has demonstrated future applications of nickel silcide nanowires on biological cell separation, field emitters, and magnetic storage.

Acknowledgements

The authors acknowledge the support from Ministry of Science and Technology through grants 100-2628-E-006-025-MY2 and 102-2221-E-006-077-MY3.

Notes and references

[a] *Department of Materials Science and Engineering, National Cheng Kung University, No.1, University Rd., Tainan City 701, Taiwan Fax: +886-6-2346290; Tel: +886-6-2757575-62920; Email: gkclu@mail.ncku.edu.tw*
[b] *Center for Micro/Nano Science and Technology, National Cheng Kung University, No.1, University Rd., Tainan City 701, Taiwan*

1. W. M. Weber, L. Geelhaar, A. P. Graham, E. Unger, G. S. Duesberg, M. Liebau, W. Pamler, C. Cheze, H. Riechert, P. Lugli and F. Kreupl, *Nano Lett.*, 2006, **6**, 2660-2666.
2. Y. Wu, J. Xiang, C. Yang, W. Lu and C. M. Lieber, *Nature*, 2004, **430**, 61-65.
3. S. Y. Chen, P. H. Yeh, W. W. Wu, U. S. Chen, Y. L. Chueh, Y. C. Yang, S. Gwo and L. J. Chen, *ACS Nano*, 2011, **5**, 9202–9207.
4. C. H. Cheng and C. L. Hsin, *CrystEngComm*, 2014, **16**, 10933-10936.
5. C. Y. Lee, M. P. Lu, K. F. Liao, W. W. Wu and L. J. Chen, *Appl. Phys. Lett.*, 2008, **93**, 113109.
6. Z. H. Liu, H. Zhang, L. Wang and D. R. Yang, *Nanotechnology*, 2008, **19**, 4.
7. D. J. Kim, J. K. Seol, M. R. Lee, J. H. Hyung, G. S. Kim, T. Ohgai and S. K. Lee, *Appl. Phys. Lett.*, 2012, **100**, 4.
8. K. C. Lu, W. W. Wu, H. W. Wu, C. M. Tanner, J. P. Chang, L. J. Chen and K. N. Tu, *Nano Lett.*, 2007, **7**, 2389-2394.
9. W. W. Wu, K. C. Lu, C. W. Wang, H. Y. Hsieh, S. Y. Chen, Y. C. Chou, S. Y. Yu, L. J. Chen and K. N. Tu, *Nano Lett.*, 2010, **10**, 3984-3989.
10. Y. C. Chou, W. W. Wu, C. Y. Lee, C. Y. Liu, L. J. Chen and K. N. Tu, *J. Phys. Chem. C*,2011, **115**, 397-401.
11. C. A. Decker, R. Solanki, J. L. Freeouf, J. R. Carruthers and D. R. Evans, *Appl. Phys. Lett.*, 2004, **84**, 1389-1391.
12. L. F. Dong, J. Bush, V. Chirayos, R. Solanki, J. Jiao, Y. Ono, J. F. Conley and B. D. Ulrich, *Nano Lett.*, 2005, **5**, 2112-2115.
13. C. J. Kim, K. Kang, Y. S. Woo, K. G. Ryu, H. Moon, J. M.

CrystEngComm Accepted Manuscript

Kim, D. S. Zang and M. H. Jo, *Adv. Mater.*, 2007, **19**, 3637-3642.
14. J. Kim and W. A. Anderson, *Thin Solid Films*, 2005, **483**, 60-65.
15. J. Kim, W. A. Anderson, Y. J. Song and G. B. Kim, *Appl. Phys. Lett.*, 2005, **86**, 3.
16. J. Kim and W. A. Anderson, *Nano Lett.*, 2006, **6**, 1356-1359.
17. Y. P. Song and S. Jin, *Appl. Phys. Lett.*, 2007, **90**, 3.
18. Y. P. Song, A. L. Schmitt and S. Jin, *Nano Lett.*, 2007, **7**, 965-969.
19. J. Lindroos, D. P. Fenning, D. J. Backlund, E. Verlage, A. Gorgulla, S. K. Estreicher, H. Savin and T. Buonassisi, *J. Appl. Phys.*, 2013, **113**, 7.
20. D. A. Porter and K. E. Easterling, in *Phase Transformations in Metals and Alloys*, Nelson Thornes, Cheltenham, 2nd edn, 2001,
21. D. Hesse and R. Mattheis, *Phys. Status Solidi A-Appl. Res.*, 1989, **116**, 67-80.
22. R. G. Forbes, *Solid-State Electron.*, 2001, **45**, 779-808.
23. M. A. Pawlak, A. Lauwers, T. Janssens, K. G. Anil, K. Opsomer, K. Maex, A. Vantomme and J. A. Kittl, *IEEE Electron Device Lett.*, 2006, **27**, 99-101.
24. J. A. Kittl, M. A. Pawlak, A. Lauwers, C. Demeurisse, K. Opsomer, K. G. Anil, C. Vrancken, M. J. H. van Dal, A. Veloso, S. Kubicek, P. Absil, K. Maex and S. Biesemans, *IEEE Electron Device Lett.*, 2006, **27**, 34-36.

CrystEngComm Accepted Manuscript

This journal is © The Royal Society of Chemistry [year]

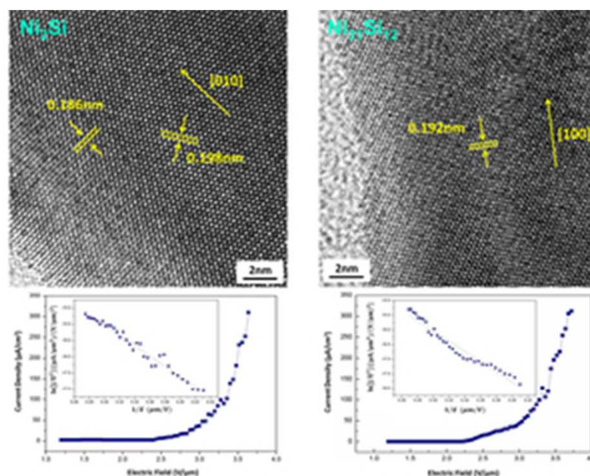

Single-crystalline NiSi2, Ni2Si and Ni31Si12 nanowires with outstanding characteristics were synthesized through nickel transported chemical vapor deposition method.
39x19mm (300 x 300 DPI)

CrystEngComm Accepted Manuscript